aerospace

MDPI

Article

Analysis Leading to the Design of a Hybrid Gas-Electric Multi-Engine Testbed

Agata Kuśmierek [1], Rafał Grzeszczyk [2], Andreas Strohmayer [3] and Cezary Galiński [1,*]

[1] Faculty of Power and Aeronautical Engineering, Warsaw University of Technology, 00-665 Warsaw, Poland; agata.kusmierek.dokt@pw.edu.pl
[2] ODIUT Automex Sp. z o.o., 80-557 Gdańsk, Poland; rafal.grzeszczyk@automex.eu
[3] Institute of Aircraft Design, University of Stuttgart, 70550 Stuttgart, Germany; strohmayer@ifb.uni-stuttgart.de
* Correspondence: cezary.galinski@pw.edu.pl

Abstract: Given the increase in air traffic, the main challenges in aircraft design are in-flight emissions and noise heard by the community. These problems have thus far been solved by incremental improvements in aerodynamics, engine technology and operation. To dramatically reduce aviation's carbon footprint towards an environmentally friendly air transport system, alternative propulsion concepts are one of the promising areas of research and first applications. In this context, the goal of integrating a hybrid-electric powertrain with a suitable airframe is to increase efficiency while reducing in-flight emissions, reduce noise for the community, drive down direct operating costs and increase reliability. This article presents an inexpensive approach to testing small, manned aircraft with a hybrid fuel–electric propulsion system. First, the design assumptions of the research flying platform are presented. Next, modifications of the existing two-seater glider are analyzed. These modifications are necessary to fit the fuel–electric hybrid propulsion system. The analysis allows us to select the elements of an appropriate hybrid electric system. It also shows that this type of small experimental propulsion system can be mounted on a two-seater aerobatic glider without significant structural modifications and still comply with the most important points of the Certification Standard-22. Finally, the design of the ground test stand for the propulsion system is described. It is believed that a thorough examination of the propulsion system on the ground will reveal both the advantages and disadvantages of the system. This should facilitate the successful installation of the system under study on a flying aircraft.

Keywords: hybrid fuel–electric propulsion system; motor glider; ground testbed

Citation: Kuśmierek, A.; Grzeszczyk, R.; Strohmayer, A.; Galiński, C. Analysis Leading to the Design of a Hybrid Gas-Electric Multi-Engine Testbed. *Aerospace* **2023**, *10*, 998. https://doi.org/10.3390/aerospace10120998

Academic Editor: Stephen Whitmore

Received: 20 October 2023
Revised: 11 November 2023
Accepted: 18 November 2023
Published: 28 November 2023

1. Introduction

With respect to air traffic growth in Europe, in-flight emissions and community noise are a major challenge to aircraft design, up to now essentially addressed with incremental improvements in aerodynamics, engine technology and operations. In the effort to dramatically reduce the carbon footprint of aviation for an environmentally friendly air transport system, as requested by the European Green Deal [1] and supported by the Advisory Council for Aviation Research and Innovation (ACARE) in the "Fly the Green Deal, Europe's Vision for Sustainable Aviation" report [2], alternative propulsion concepts are one of the promising fields for research and first applications. In this context, the objective of the integration of a hybrid-electric propulsion system in a suitable airframe is to increase efficiency while reducing in-flight emissions, reduce community noise and the viable operating cost and increase reliability.

In view of emissions, aircraft ideally would be fully electric, but given the limited range and endurance of battery-powered aircraft due to the limited specific energy capacity of current battery technologies, this is not viable for commercial air transport and similar applications. As the gravimetric energy density of today's typical lithium-ion cells is

about 45 times lower than the energy density of conventional fuel, all-electric power train architectures suffer from a significant mass penalty. However, the advantage of fuel can be combined with the advantage of the electric airframe with its synergistic configuration potential and thus provide improved aerodynamic qualities by designing a hybrid electric aircraft. Using energy for the flight mission from batteries can be beneficial for the overall primary energy consumption of a hybrid-electric aircraft, but in view of the use case and the power split in each mission segment, it must be ensured that carrying battery capacity proves beneficial for the overall energy balance.

The application of hybrid-electric propulsion together with synergistic effects proves to be a promising solution, in particular in the general aviation sector. Therefore, the feasibility of hybrid-electric propulsion was initially demonstrated with small general aviation aircraft with up to four seats. In 2011, Siemens, European Aeronautic Defence and Space Company (EADS) and Diamond Aircraft fitted a DA-36 with a serial-hybrid powertrain. Fuel consumption and related emissions on the DA-36 e-Star were claimed to be reduced by up to 25% [3]. Siemens then in 2018 flew its hybrid-electric Magnus eFusion, combining a SP55D electric motor with a FlyEco Diesel engine [4]. In an EU-funded project, the serial-hybrid HYPSTAIR ground test installation platform was built in 2016 under the lead of Pipistrel, also to define certification standards for such powertrain architectures [5]. In the follow-on H2020 project Modular Approach to Hybrid Electric Propulsion (MAHEPA), two variants of a serial hybrid powertrain were integrated into a Pantera airframe [6] and flight-tested in 2021. Also in 2021, the University of Stuttgart's e-Genius high-performance hybrid (HPH) had its first flight, converted from the 2011 battery-electric e-Genius with a serial-hybrid powertrain, based on a three-cylinder turbocharged multifuel engine and an axial flux permanent magnet synchronous electric machine [7]. In August 2022, the e-Genius HPH set a world record for hybrid-electric aircraft, flying 2004 km nonstop at an average speed of 191 km/h, using only 81 L of fuel with two passengers on board. Furthermore, in a project funded by the German Ministry of Economy and Energy (BMWi), the e-Genius HPH's serial-hybrid powertrain architecture was expanded to a twin demonstrator platform in 2022 in cooperation with APUS Aeronautical Engineering GmbH and Steinbeis Flugzeug- und Leichtbau GmbH [8].

In November 2018, Diamond Aircraft together with Siemens managed to fly the first hybrid-electric multi-engine application, the hybrid electric multi-engine plane (HEMEP), in a project jointly funded by BMWi and the Austrian Ministry for Transport, Innovation and Technology (BMVIT). The project aimed at reducing fuel consumption, as well as the noise footprint, with the hybrid-electric powertrain extending endurance up to 5 h [9]. In a push–pull configuration, Ampaire flew the first hybrid-electric test platform Ampaire Electric EEL in 2019. It is based on the Cessna 337 Skymaster, with the aft engine replaced by an electric motor, and claimed to have 50–70% savings in fuel consumption and 25–50% in maintenance cost [10]. As a next step towards larger applications, Ampaire brought a hybrid-electric Eco Caravan to its first flight in November 2022 [11]. VoltAero's Cassio 1 testbed aircraft, also a modified Cessna 337 Skymaster, had its first flight in early 2020. It is equipped with two forward-facing electric motors on the wings, together with an aft-mounted internal combustion engine [12]. In February 2022, the National Research Council Canada (NRC) also flew this aircraft type as a hybrid electric test platform [13].

Today, these efforts based on conventional internal combustion engines are supplemented by power trains based on hydrogen and fuel cells. The first demonstration of this powertrain architecture was already made in 2008 by Boeing Research and Technology Europe in Madrid, converting a two-seat Dimona motor glider with a proton exchange membrane (PEM) fuel cell combined with a lithium-ion battery system to power an electric motor [14]. In September 2016, the HY4 demonstrator had its first flight, a conversion of the previously all-electric Pipistrel Taurus G4 with a fuel cell, led by DLR in Stuttgart. In 2022, the HY4 reached an altitude of 7230 ft [15]. Only recently, this was followed by larger commuter aircraft conversions, such as ZeroAvia's Do228 testbed [16] and the Universal Hydrogen Dash-8 [17]. In both demonstrator architectures, one side of the twin

arrangement is converted with a fuel cell system, while the other side still works on the conventional propulsion system.

All of this work, up to now mainly focused on smaller general aviation aircraft, can demonstrate the effects of hybrid-electric architectures on key factors such as fuel consumption, noise and maintenance efforts and will help to de-risk the development of larger aircraft, which, once in operation, will obviously have a more significant environmental impact.

2. Motivation and Objective

Despite the more significant environmental impact of large commercial aircraft, the development of hybrid electric propulsion systems for small aircraft remains important. Despite the development of flight simulator technology, training on small airplanes is still the most effective method of training pilots of commercial passenger aircraft. Therefore, the fleet of small airplanes will remain large until unmanned commercial aircraft can carry passengers. Unfortunately, outdated piston engines designed in the 1950s (with minor modifications) still power the propellers of many small aircraft used for training. All of these airplanes can be replaced with new ones with the advanced propulsion systems currently developed and tested. This will not only drive down general aviation emissions but also teach pilots how to use these new propulsion systems. This knowledge will then be useful in the course of pilots' careers in commercial aviation also utilizing the new generation of propulsion systems.

The topic of aeronautical hybrid electric propulsion systems is thoroughly summarized in several review papers [18–21], and new interesting works are frequently emerging [22–29]. The main purpose of this paper is to present the methodology of designing a hybrid, gas–electric multi-engine propulsion system implemented by the Warsaw University of Technology. This propulsion system is installed on the ground testbed for an investigation. However, it was designed so that in the future the tested propulsion system could be mounted on the PW6A [30] acrobatic glider and tested in flight. The purpose of this experiment is to demonstrate the possibility of using a hybrid, gas–electric multi-engine propulsion system in the PW-X20 hybrid motor glider (utility category), conduct tests and gain knowledge about hybrid drive systems. The mission profile of this aircraft is limited to take-off, climb, cruise (with battery recharging) and landing.

Assumptions:

- Conversion of the PW6A glider with a front electric sustainer (FES) into the hybrid gas–electric twin-engine PW-X20 motor glider;
- Reduction in the crew to only one passenger;
- Maximum take-off mass (MTOM) < 850 kg;
- As few modifications as possible in the aircraft's structure;
- 5 min of climbing with batteries only;
- 2 h flight with the internal combustion engine (ICE);
- 5.5 m/s climb rate at full power;
- Positive climb rate on batteries only.

The following modes of propulsion operation were assumed in normal conditions:

- Take-off performed with both the power generator and batteries working together.
- Initial climbing performed with both the power generator and batteries working together.
- Extended climbing performed with the power generator supplying propeller motors with the simultaneous cooling of the batteries.
- Cruise performed with the power generator supplying motors driving propellers and simultaneously recharging the batteries.

Moreover, two emergency modes were predicted:

- In the case of a battery malfunction, the PW-X20 should have a positive climb rate with power delivered from the ICE only.

- In the case of a power generator malfunction, the PW-X20 should have a positive climb rate with power delivered from batteries only and batteries' capacity large enough to perform at least one circle to land round.

3. Sizing and the Concept of the Propulsion System

The characteristics of the propulsion system were defined by analyzing the performance of the envisaged twin-propeller motor glider. This informed the decision on the performance of the power generator and electric motors used to drive propellers, as well as the number of lithium cells necessary to achieve the assumed flight endurances. Selected components of the propulsion system were then arranged in a way to minimize the number of necessary modifications of the baseline platform.

3.1. Aerodynamic Characteristics

The aerodynamic characteristics of the wing were calculated based on two different methods. First, wind tunnel tests performed for the NN 18-17 airfoil were used in order to calculate the aerodynamic characteristics of the wing analytically. The airfoil NN 18-17 is a gently modified version of the airfoil NN 17-17. Both airfoils were designed in the late 1980s, quite probably without advanced CFD analysis (at least this analysis is not available for the authors at the moment). Anyway, recently we have calculated the characteristics of NN 18-17 with XFOIL to see the difference between wind tunnel tests and the calculated characteristics. Comparison of these characteristics can be seen in Figure 1. Quite good agreement can be observed in the most interesting range of lift coefficients (0.6–1.35). Both characteristics reveal nonmonotonic behavior of the drag coefficient with respect to the lift coefficient for positive values of the lift coefficient. For the first view, it might look strange since monotonic growth could be expected. However, one should remember that the monotonic growth of the drag of the wing mainly results from the induced drag component which is inversely proportional to the aspect ratio. In the case where an airfoil infinite aspect ratio is assumed, the induced drag is equal to zero, thus reducing the tendency to monotonicity. In the case of wind tunnel test, infinite aspect ratio was simulated by measurement in the closed measurement section of the tunnel, the model was extending from one wall of the tunnel to the opposite wall of the tunnel. Lift and drag coefficients were measured in the plane of symmetry from pressure distributions on the airfoil and in the wake [31]. On the other hand, many sources claim that the minimum drag of the airfoil occurs for Cl = 0 only for symmetrical airfoils. In the case of asymmetrical airfoils, the minimum of the drag is shifted to positive values of Cl and the shift depends on the curvature of the camber line, e.g., [32–34]. NN 18-17 is highly cambered so the minimum of the drag for the positive Cl is normal.

The analytic method of the lift and drag calculation was based on the assumption that the taper ratio is constant (differences in tip geometry were omitted). The characteristics were calculated taking into account the Reynolds number, the wing's material (composite) and Glauert's correction. The results were compared with AOS-71—electric motor glider (utility category)—wing wind tunnel tests [35] in plain configuration due to a lack of similar data from the PW6A wind tunnel tests. This simplification could be made because the AOS-71 wings differ only slightly from the PW6 wings (the AOS-71 has speed flaps whereas the PW6A does not). It turned out that the lift coefficient (Cl)–angle of attack (AOA) curves are almost the same for both methods (Figure 2). For the lift–drag diagram, the minimum drag was almost at the same point, but there was a noticeable difference for the higher lift coefficients (Figure 3). Therefore, the worse scenario was assumed, and the AOS-71 wind tunnel data were used for further calculations.

The aerodynamic characteristics of the aircraft were calculated, including the standard configuration of the PW6A glider (fuselage, landing gear, vertical and horizontal stabilizer, etc.), as well as the new equipment resulting from hybrid gas–electric double engine propulsion. Parasite drag coefficients are presented in Table 1.

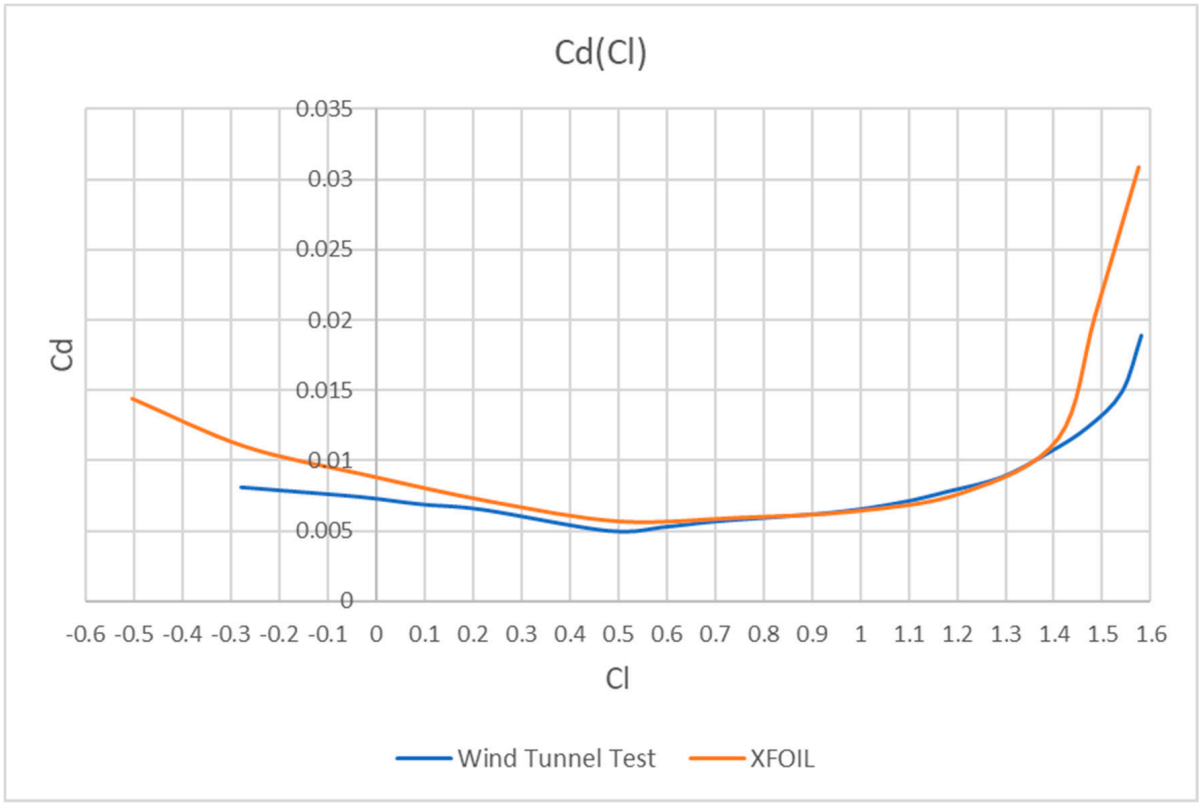

Figure 1. Comparison of NN 18-17 CFD calculations and wind tunnel tests.

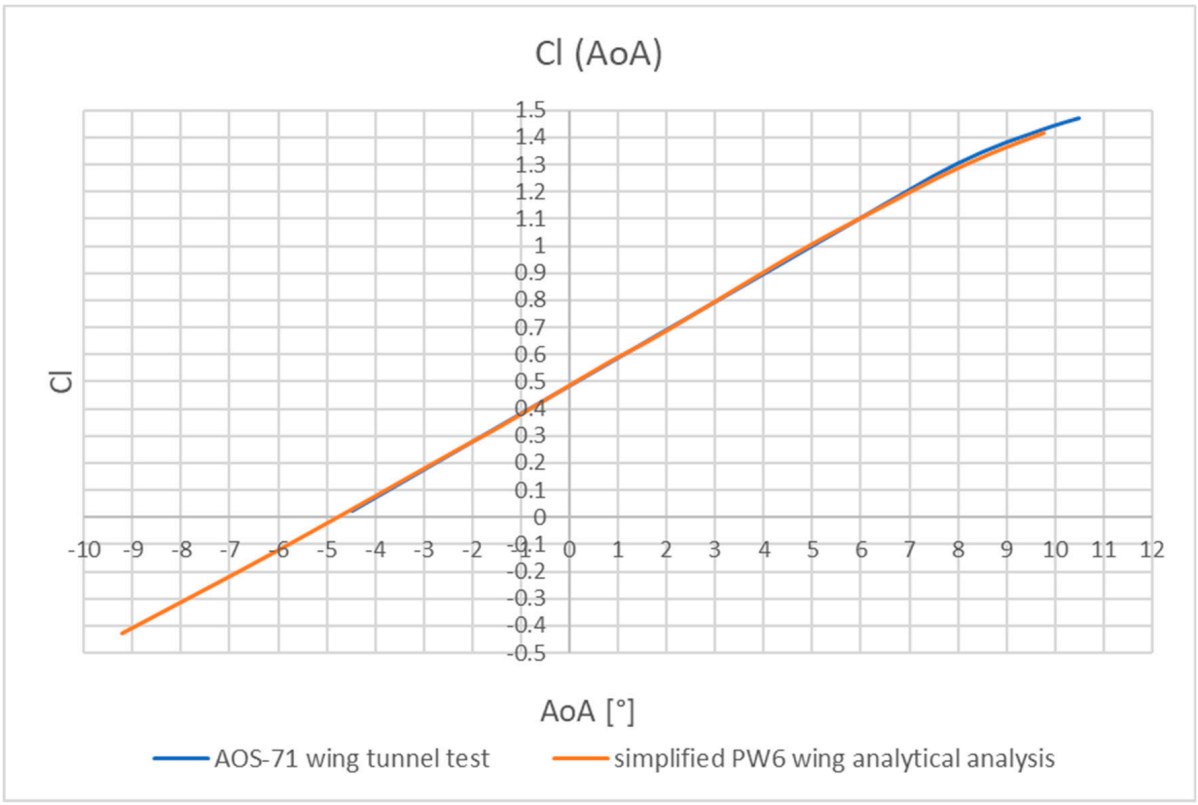

Figure 2. Graph of the lift coefficient (Cl) versus angle of attack (AoA) for the PW-X20 wing—the comparison between two calculation methods.

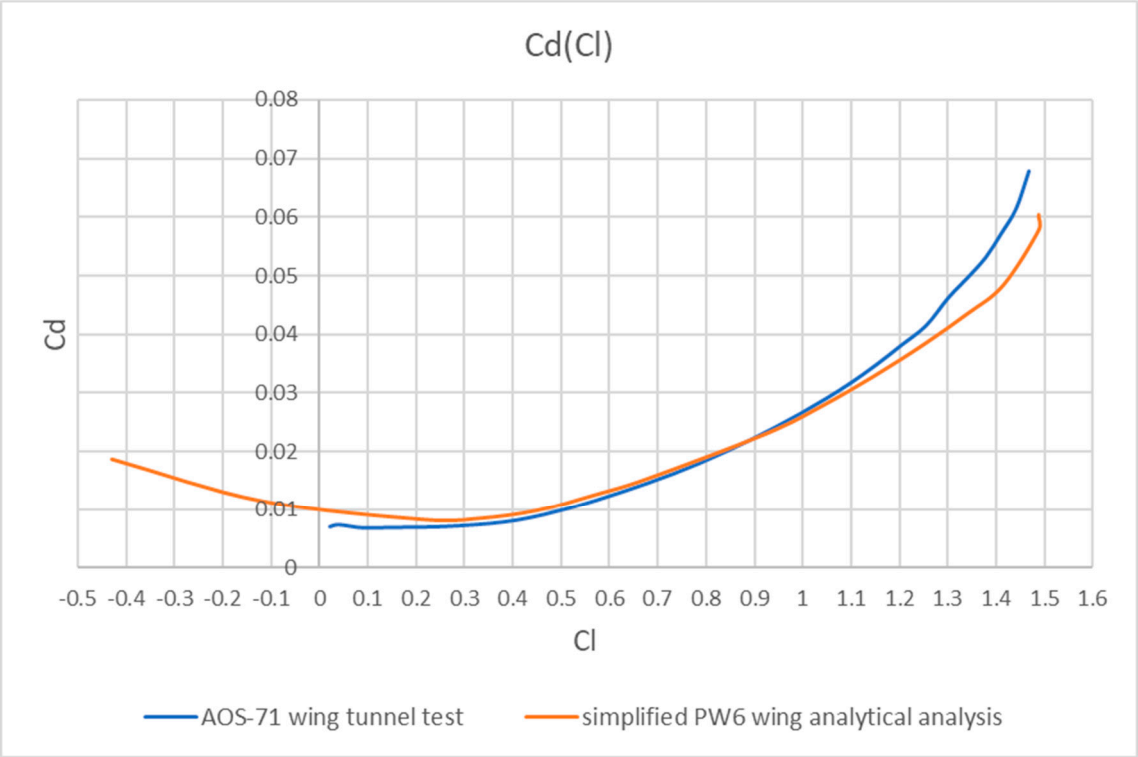

Figure 3. Graph of the drag coefficient (Cd) versus lift coefficient (Cl) for the PW-X20 wing—the comparison between two calculation methods.

Table 1. Parasite drag in reference to the wing reference area.

	Cd_i
Fuselage	0.002797
Horizontal stabilizer	0.00059–0.000951 (Cl dependency)
Vertical stabilizer	0.00059
Motors' nacelles	0.000787
Generator's nacelle	0.00059
Main landing gear	0.000131
Front landing gear	0.0000656
Rear wheel	0.000033
Other (inlets, gaps, etc.)	0.0088

Additional drag was generated by the power generator set consisting of the ICE with the integrated electric motor placed at the top of the fuselage; the area behind the crew cabin in the fairing (Figure 4, No. 1); two battery sets in the nacelles mounted in front of the leading edge of the wing (Figure 4, No. 2); two pylons with electric motors, and pushing propellers behind the trailing edge of the wing in line with the battery sets (Figure 4, No. 3). The added propulsion system reduced the PW6 maximum lift-to-drag ratio from 34 (for the PW6A glider configuration) down to 23 (for the hybrid PW-X20 configuration). The drag–lift coefficient diagram is presented in Figure 5.

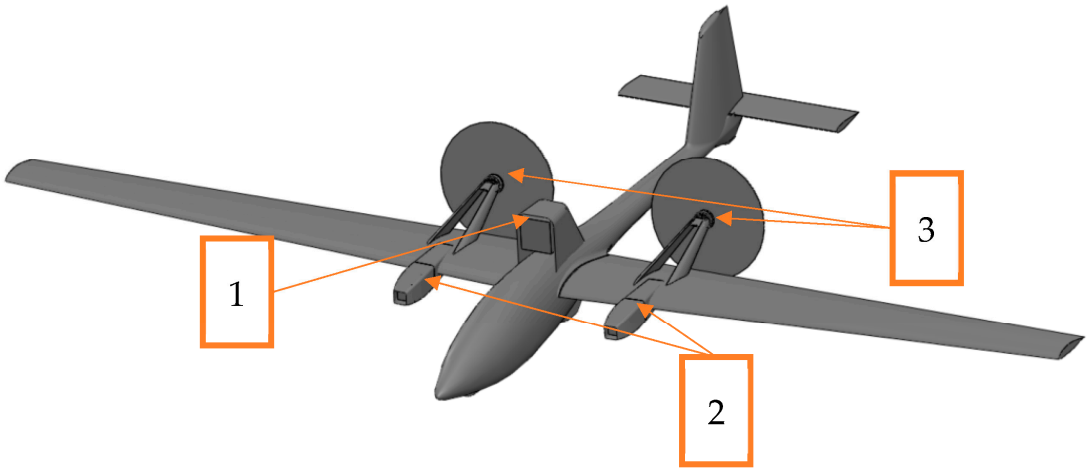

Figure 4. Visualization of the PW-X20 motor glider with the hybrid gas–electric multi-engine propulsion. (1) Power generator, (2) nacelles with batteries and converters, (3) electric motors with propellers.

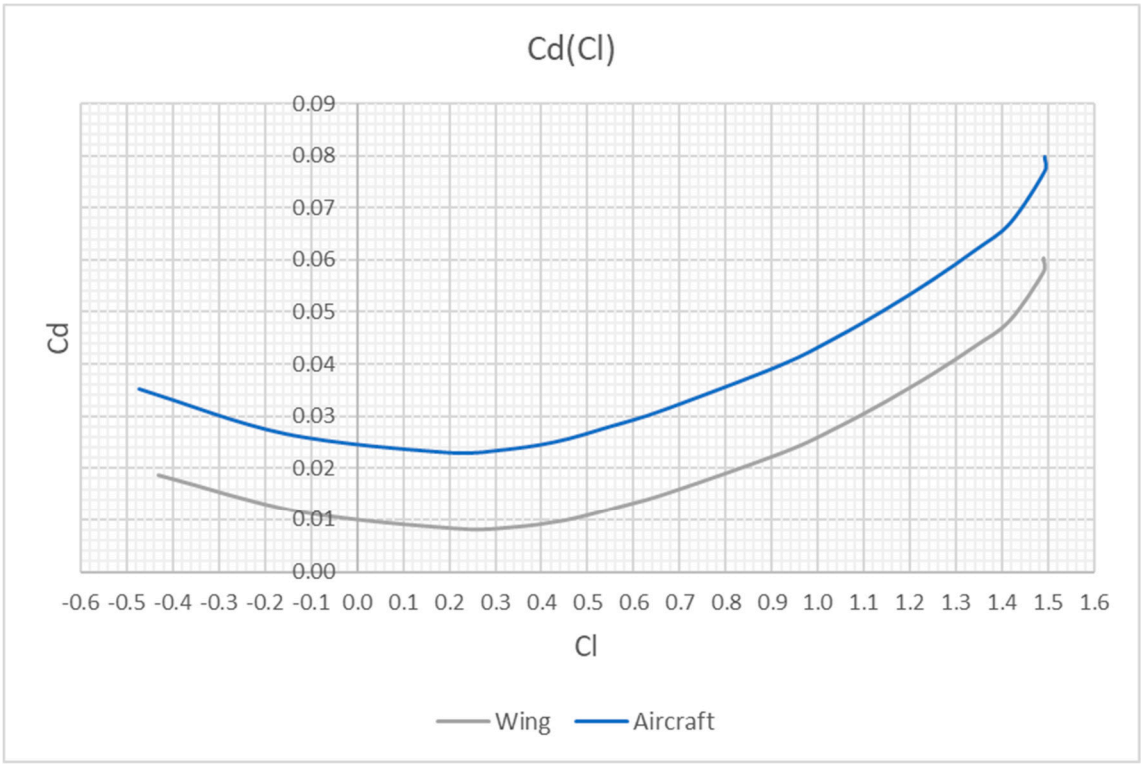

Figure 5. Graph of the drag coefficient (Cd) versus the lift coefficient (Cl) for the airfoil wing and hybrid PW6 aircraft.

3.2. Power Requirement

The required maximum take-off power was calculated based on the following formula:

$$P_{required} = P_{horizontal\ flight} + P_{climbing} = \frac{m_{aircraft} \cdot g \cdot v_{max}}{K} + m_{aircraft} \cdot g \cdot w \quad (1)$$

where:

g—Gravitational acceleration;
K—Maximum lift-to-drag ratio;
$M_{aircraft}$—Mass of aircraft;

$P_{climbing}$—Required power for climbing;
$P_{required}$—Required power;
$P_{horizontal\ flight}$—Required power for horizontal flight;
V_{max}—Maximum speed;
w—Climbing speed.

The mass of the aircraft was assumed as equal to the maximum allowed mass of the motor glider according to CS-22 regulations [36]. Taking into account the propulsive unit efficiency, the power required to supply each electric motor was established at 36.5 kW. This power should be provided by the power generator and batteries working together. Various ICEs available on the market were considered to create a design of the power generator.

Assuming the power of the ICE P_{ICE} and the flight time on the batteries $t_{battery}$, the energy of the batteries $E_{battery}$ could be calculated as:

$$E_{battery} = \left(P_{required} - P_{ICE}\right) \cdot t_{battery} \quad (2)$$

Then, using the specific energy of typical lithium polymer batteries, the parameters of the batteries were estimated. Since the envisaged time of flight using batteries is very limited, there was no need to search for batteries with a very high specific energy. Moderate battery performance should also have a positive effect on reliability and safety. Consequently, standard commercially available cells with a gravimetric energy density of approximately 140 Wh/kg are going to be used.

Finally, the Hirth 3503 [37] was selected as the ICE and supplemented with a water-cooled low-voltage EMRAX 268 [38] motor to create a power generator. Air-cooled high-voltage EMRAX 228 [39] motors were selected to drive the propellers. It was also decided that 240 US18650VTC6 [40] or similar cells would be necessary to perform the assumed mission safely. The cells would be assembled in two batteries (Figure 6). The batteries would be connected in parallel while the cells inside each battery would be connected in series, i.e., each of the two batteries would contain 120 cells connected in series. The work in [40] recommends charging cells to 4.15 V to obtain the best cycle life performance. Therefore, the maximum voltage of one battery would be equal to 498 V. Two batteries connected in parallel would have the same maximum voltage. This would be the voltage experienced by the motor just after the battery was connected; therefore, the motor would be safe. The work in [40] also recommends not to exceed 20 A during the discharge of the single cell. A total of 120 cells connected in series should have the same discharge current. However, two such batteries connected in parallel would allow us to draw 40 A from this system of batteries. For safety reasons, it was assumed that the temperature during discharge should not exceed 80°. According to [40], this temperature could be achieved during the continuous discharge of a single cell by 20 A when the voltage falls from 4.2 V to approximately 3 V. During such a discharge, the cell would deliver 2.4 mAh. Such a discharge could happen in the case of ICE malfunction during take-off. In this case, both batteries could still provide up to 19.7 kW of power available to fly just before the batteries cut off, assuming an efficiency of the propeller equal to 80%, an efficiency of the motors equal to 95% and an efficiency of the power distribution system equal to 90%. At the same time, the smallest power required to fly would be approximately equal to 9.7 kW. This gives approximately 10 kW of excess power and a climb rate of 1.36 m/s. On the other hand, 2.4 mAh from each cell in both batteries would allow the propulsion system to operate for 7.2 min assuming a current of 20 A. This means that at least 7.2 min of continuous climbing would be available after ICE malfunction which exceeds the assumed value of 5 min of continuous climbing. Therefore, the circle to land round maneuver could be performed with a current smaller than 20 A, which proves that the design of the batteries would be safe.

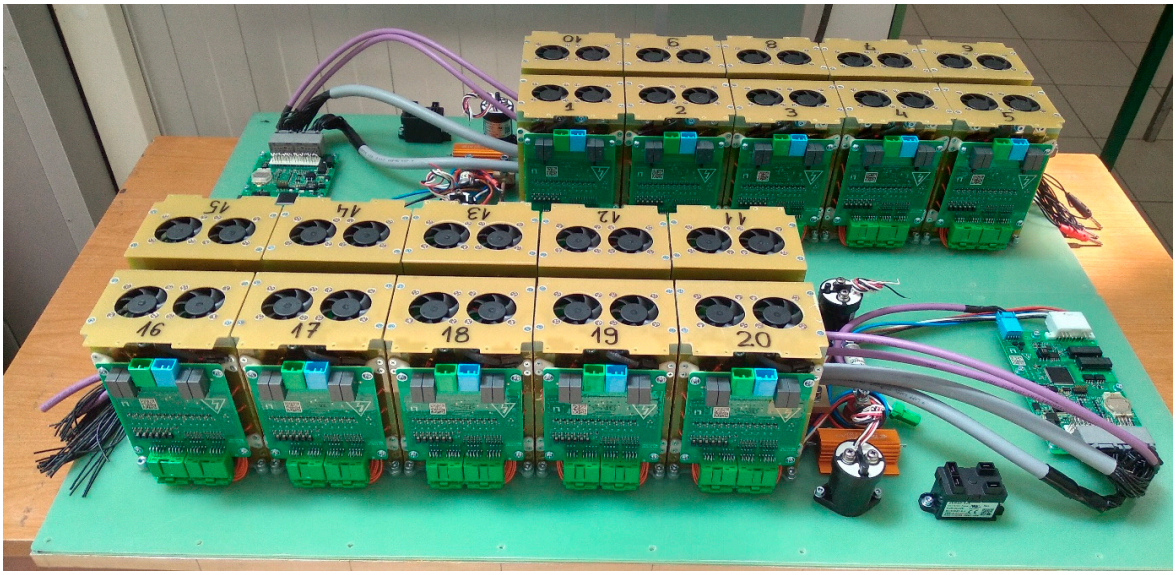

Figure 6. Batteries suitable for PW-X20 aircraft. Note the significant share of the battery management systems (BMS) and cooling systems in the battery mass.

Considering different ways of power distribution (ICE only, batteries only, ICE + batteries, ICE + batteries recharging), the propulsive unit characteristics were analyzed. The calculations show that due to the complicated nature of power distribution, a fixed-pitch propeller is not the right choice for hybrid propulsion. It seems impossible due to great differences between the power required for the different flight modes and between the power available in different modes of propulsion operation. The very wide range of blade pitch angles have to be found (up to 40–45 degrees) in order to satisfy the assumed available and required powers in the case of fixed-pitch propellers. Nevertheless, such a propeller may be found or designed; however, it will have a very poor performance in every flight mode. This issue will be investigated in further experiments conducted on the testbed. They will be performed with various propellers with a diameter of 1.3 m, both two-bladed and three-bladed. First, propellers to be tested are serially manufactured and frequently applied, e.g., for motorized paraplanes. They consist of composite blades and hubs allowing for pitch adjustment (assuming that the propeller is removed from the motor). This will allow for propulsion testing with several different propeller characteristics.

3.3. Mass Distribution and Strength Analysis

As the components of the hybrid propulsion were finally chosen, a great deal of effort was made to locate parts of the hybrid propulsion in the existing PW6 airframe so that the glider's center of mass (CoM) would not go beyond the allowed limits.

As per CS-22 regulations, the maximum mass was envisaged at 850 kg. With the mass of the aircraft increasing due to the use of hybrid gas–electric propulsion, the decision was made to limit the crew from two to only one pilot. Therefore, the aft pilot's place would be used for the gasoline tank in such a way that the gasoline consumption during the flight would not significantly change the aircraft's CoM in the X direction. Placing fuel in the fuselage also helps to isolate the fuel tank and pipes from high-power electric wires. What is more, this location simplifies the design of the fuel system, since there is no need to run the pipes through removable wings.

Similarly, for the generator set of a total mass of 65 kg, the location near the aircraft's CoM was chosen. Unfortunately, even if the Hirth engine as an ICE and the Emrax motor were chosen due to their small size, the overall dimensions of the generator set (including gearbox, cooling and exhaust systems) are quite large. Due to space constraints in the existing aircraft's airframe, as well as safety considerations, it was decided to install the

generator set on the top of the fuselage (Figure 4, No. 1) on a specially designed engine bed covered with a fairing to reduce the drag. This was possible because the original PW6U glider (utility category) [30] design contained additional fitting points at the top of the fuselage for research purposes [41,42].

It was decided to place the batteries in the nacelles mounted in the front of the leading edge, symmetrically on both wings (Figure 4, No. 2). The battery beds with the fairings are as front-ended as possible to keep the CoM toward the front of the aircraft. On the other hand, due to safety reasons, batteries should not be located close to the pilot's cabin in the event of fire in the battery compartments. The design also incorporated mechanical protection from spontaneous battery ignition. A mechanical jettison system was included in the nacelles, which can be activated by the pilot in the event of fire. Converters are also going to be mounted inside the nacelle so as not to interfere with the onboard equipment.

Safety reasons (concerns about the uncontrolled operation of an electric motor before the crew boards the glider) led to the decision to place the electric motors and propellers behind the trailing edge. They are placed symmetrically on both wings, in line with the batteries. The distance from the motors to the center of mass should be as small as possible to maintain the correct position of the CoM. However, the flow around the wing had to be taken into consideration as well. If the propeller is too close to the trailing edge, it is located in both low- and high-pressure areas, thus creating vibrations. Consequently, the distance between the trailing edge and the propeller should be at least 0.5 m based on previous experiences [43]. Both the vertical and horizontal position of the motor also depend on the diameter of the propellers. However, the yawing moment coming from a motor in the event of one motor failure was considered as well. These considerations led to the final location, which is presented in Figure 4 (No. 3). The figure also shows one of the possible methods of mounting electric motors to the wing.

The mass of electric wires was also included, since hybrid propulsions consist of many components (such as DC/AC converters, motors, batteries, etc.) and due to the high current used to power the aircraft, the mass of wires may have a significant impact on the mass of the aircraft. The mass and location of the test instrumentation were also added to the analysis. Due to the overall increase in aircraft mass and the resultant need to redesign and reinforce the landing gear, its mass is expected to grow. Similarly, the horizontal stabilizer has to be redesigned due to the CoM change in the Z direction and operation in the propeller stream. Also, the design involves the use of the Galaxy GRS 6 750 [44] rescue system for the aircraft.

Last, but certainly not least, are the wings. The original PW6A acrobatic wings were designed for a load factor of +7/−5, while the mass of the aircraft was equal to 590 kg. The idea was to decrease the load factor as much as necessary for the new and heavier PW-X20 hybrid aircraft to be able to fly. As it was outlined at the beginning of the paper, only small changes in the PW6A wing structure are acceptable. These changes include additional reinforced ribs for mounting the propulsion components and an additional layer of carbon fabric between the fuselage and this rib to carry additional torque generated by the nacelle with the battery, converter, motor mount and motor with the working propeller. The bending moment of the wings with the new equipment was calculated to ensure that any other changes in the wing structure were not necessary. Load analysis proved that the structure is strong enough to ensure the flight of the modified aircraft with the load factor decreased to +5.3/−2.65, which fits into the utility category of sailplanes according to CS-22. The wings of the aerobatic PW6A generate the lift force of $7 \times 590\ \text{kg} \times 9.81\ \text{m/s}^2 = 40{,}515.3\ \text{N}$ or $-5 \times 590\ \text{kg} \times 9.81\ \text{m/s}^2 = -28{,}939.5\ \text{N}$. Assuming load factors of the utility category, the same lift forces would be achieved for the following MTOM $40{,}515.3\ \text{N}/(5.3 \times 9.81) = 779.2\ \text{kg}$ and $-28{,}939.5\ \text{N}/(-2.65 \times 9.81) = 1113.2\ \text{kg}$. At the same time, mass analysis revealed that PW-X20 with all of the necessary modifications should have an MTOM not exceeding 750 kg. Therefore, the bending moment acting on the wing would be smaller for PW-X20 with an MTOM = 750 kg and a load factor of 5.3 than for PW6A with an MTOM of 590 kg and a load factor of 7. In reality, the maximum

bending moment acting on the wing of PW-X20 would be reduced further because the additional mass of the nacelle with the battery, converter, motor mount and motor with the propeller generate inertial force in the opposite direction to the lift.

Altogether, the CoM location in the X direction of the new hybrid PW-X20 aircraft varies from 29 to 40.5% of the mean aerodynamic chord (MAC). This result is satisfying because the PW6U glider was examined in flight for the CoM varying from 17 to 41% of the MAC. This means that changes in the propulsion do not affect the center of mass location along the wing chord. The range of CoM of PW-X20 would be inside the range of CoM of PW6U. Therefore, the effect of CoM travel on flight characteristics would be smaller for PW-X20 than for PW6U. The MTOM increased from 590 kg (2-passenger acrobatic motor glider) to about 750 kg (1-passenger hybrid aircraft). This leaves a fairly large margin for underestimations in the analysis, since the CS-22 airworthiness regulation constrains the MTOM to 850 kg for motor gliders and the maximum MTOM calculated for the load factor of 5.3 is equal to 779.2 kg. Since there are no high lift devices in the PW6 glider, the impact of the CoM on the effectiveness of their controls was not calculated.

4. The Propulsion System and Its Ground Testbed Design

Following all the analyses discussed above, it was decided that the PW-X20 hybrid propulsion would be designed in a series configuration (Figure 7) and would consist of:

- A generator set consisting of the Hirth engine series 3503 (ICE) and an AC electric motor cooled by combined liquid and air (Emrax 268);
- 2 electric motors cooled by air (Emrax 228);
- 2 propellers;
- 2 batteries, 15 kg each plus 5 kg for BMS and cooling system;
- Additional equipment (converters, gearbox, etc.).

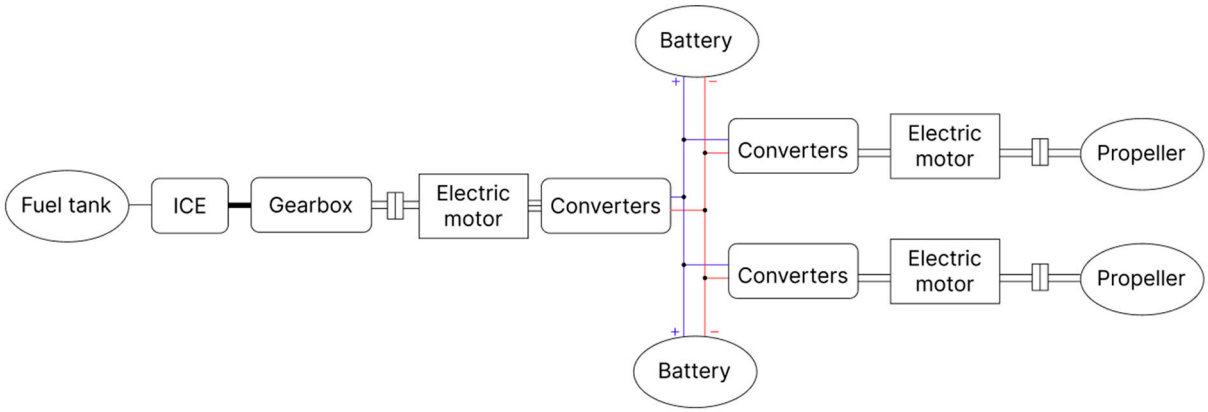

Figure 7. Series architecture of the PW-X20 hybrid aircraft.

The motors selected for this prototype aircraft are designed and manufactured by the Emrax company, with model 228 being selected for driving the propellers and model 268 for the power generator driven by an internal combustion engine. The decision to use permanent magnet synchronous motors (PMSM) was a result of their outstanding performance, including their torque/power-to-mass ratio, compact size and efficiency.

Selected parameters of the motor model chosen to drive the propellers of this experimental aircraft are listed in the following Table 2 and presented in Figures 8 and 9.

There are different motor variants available, characterized by three different voltages within the type portfolio. Selecting a lower voltage would result in a higher current for an identical performance, thus necessitating thicker wiring and a higher mass, which is obviously not desirable in any aviation application. This led to the choice of the high-voltage variant. There are also different cooling options available, with the air-cooled design being selected for the same reason (minimizing the mass of the system). This choice was possible because motors driving propellers experience forced flow even when the

airplane is motionless. A downside of this decision is a reduced water-resistance rating (only IP21 for the air-cooled design), which was nonetheless assessed as satisfactory at this stage of the project. Using the IP65-rated liquid-cooled version would increase the total mass and complexity of the system.

Table 2. Selected parameters for the propeller motor EMRAX228 [39].

Mechanical		**Electrical**	
Diameter/length	228 mm/86 mm	Max battery voltage	830 V *
Mass	12.9 kg *	Peak power S2 2 min (6500 RPM)	104 kW *
Stator cooling	air	Continuous power S1	55 kW *
Limiting speed RPM	6500	Peak torque	220 Nm
Rotor inertia [kgm^2]	0.02521	Continuous torque	96 Nm *
		Efficiency	92–98%
		Peak motor current	235 Arms *
		Continuous motor current	120 Arms *
		Number of pole pairs	10
		Winding configuration	star

* high-voltage, air-cooled variant.

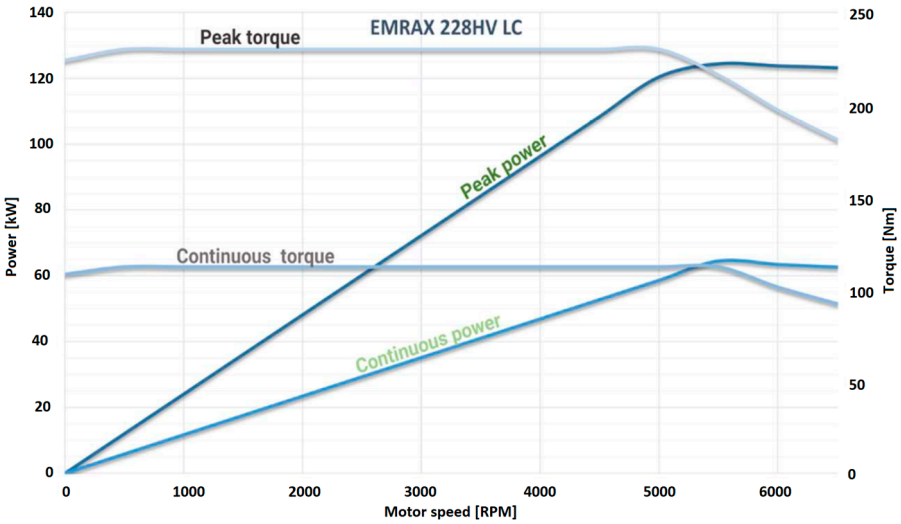

Figure 8. EMRAX228 characteristics [39].

The ICE (internal combustion engine) used in this setup is the Hirth 3503 two-cylinder in-line two-stroke liquid-cooled engine. This engine was selected for its performance characteristics, including the power-to-mass ratio and other features like the dual-ignition system. The ignition system is fully electronic and factory programmable (ignition curve). It includes a magneto, enabling it to operate whether 12 V DC from the battery is available or not. The power generator engine parameters are monitored in the control module (exhaust gas temperatures, coolant temperature, cylinder head temperature). The engine ECU communicates with the main controller via a serial interface. Apart from the Hirth3503 engine, the electric power generator also consists of an electric motor working in generator mode. The EMRAX268_LV_CC motor was adopted as the suitable model for this role due to its performance and mechanical characteristics (Table 3, Figures 10 and 11). Its design incorporates the so-called combined-cooling option, which means that it is cooled by both liquid coolant like the ICE (partially the same cooling system) and air flow. This is particularly important for ground operations of the aircraft (like taxiing and run-up) when

the required airflow cannot be guaranteed since the power generator is located out of the propeller stream.

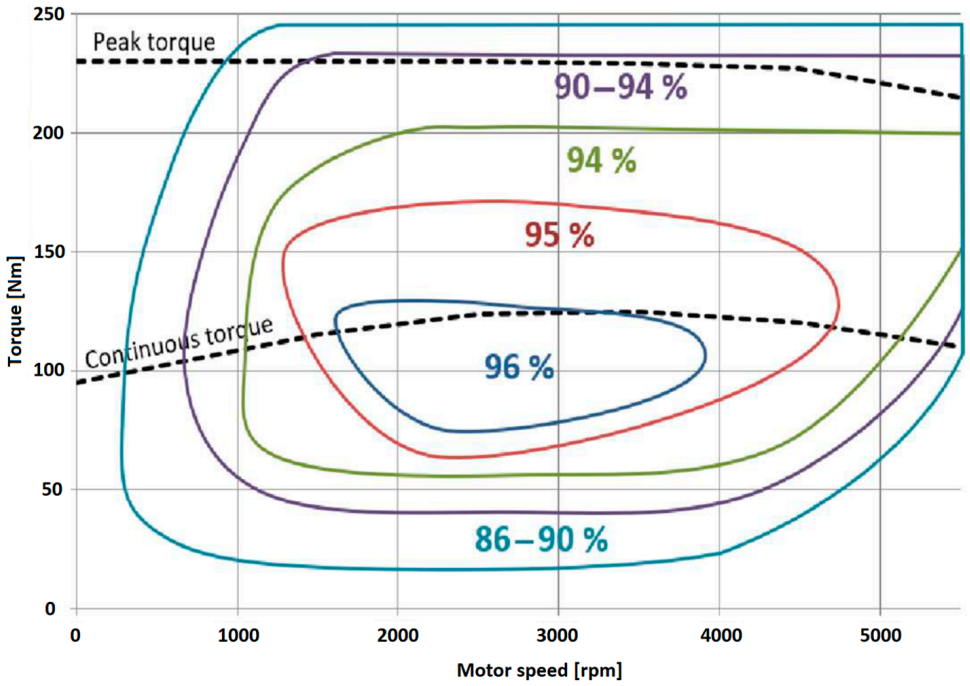

Figure 9. Efficiency of the EMRAX228 motor [39].

Table 3. Selected parameters for the generator motor EMRAX268 [38].

Mechanical		**Electrical**	
Diameter/length	268 mm/94 mm	Max voltage	340 Vdc *
Mass	21.9 kg *	Peak power S2 2 min (4500 RPM)	210 kW *
Stator cooling	combined	Continuous power S1	117 kW *
Limiting speed RPM	4500	Peak torque	500 Nm
Rotor inertia [kgm^2]	0.05769	Continuous torque	250 Nm *
		Efficiency	92–98%
		Peak motor current	1300 Arms *
		Continuous motor current	550 Arms *
		Number of pole pairs	10
		Winding configuration	star

* low-voltage, combined-cooling variant.

This time, the low-voltage variant was selected to align its voltage with voltage of completely discharged batteries and thus prevent an uncontrolled increase in current at the beginning of the charging process.

It is necessary to implement a gearbox between the internal combustion engine and the PMSM motor to use the complete working envelope of both. This is due to their different maximal rotational speeds and torque characteristics. This setup used a dedicated fixed-ratio gearbox, which was developed utilizing a toothed belt and wheels.

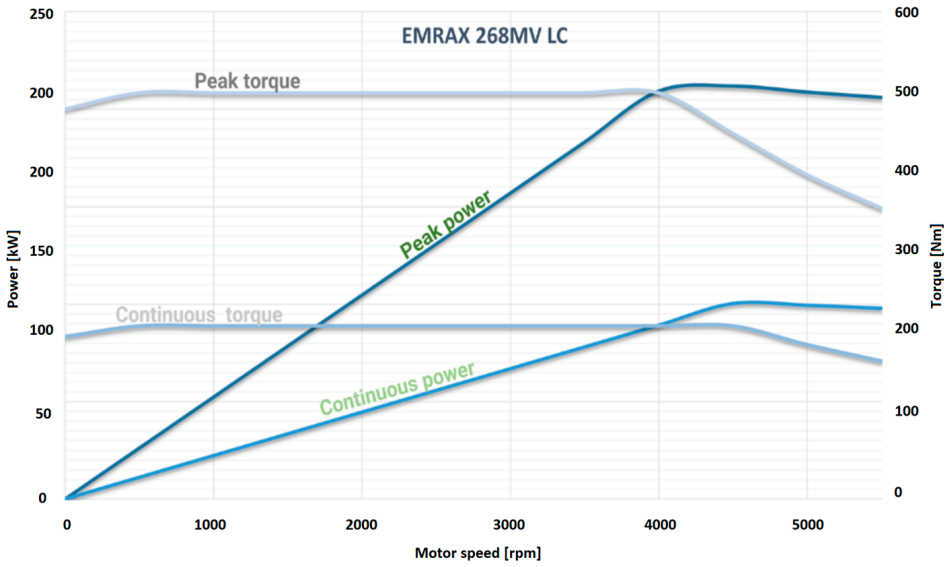

Figure 10. Torque and power curves of the EMRAX268 motor [38].

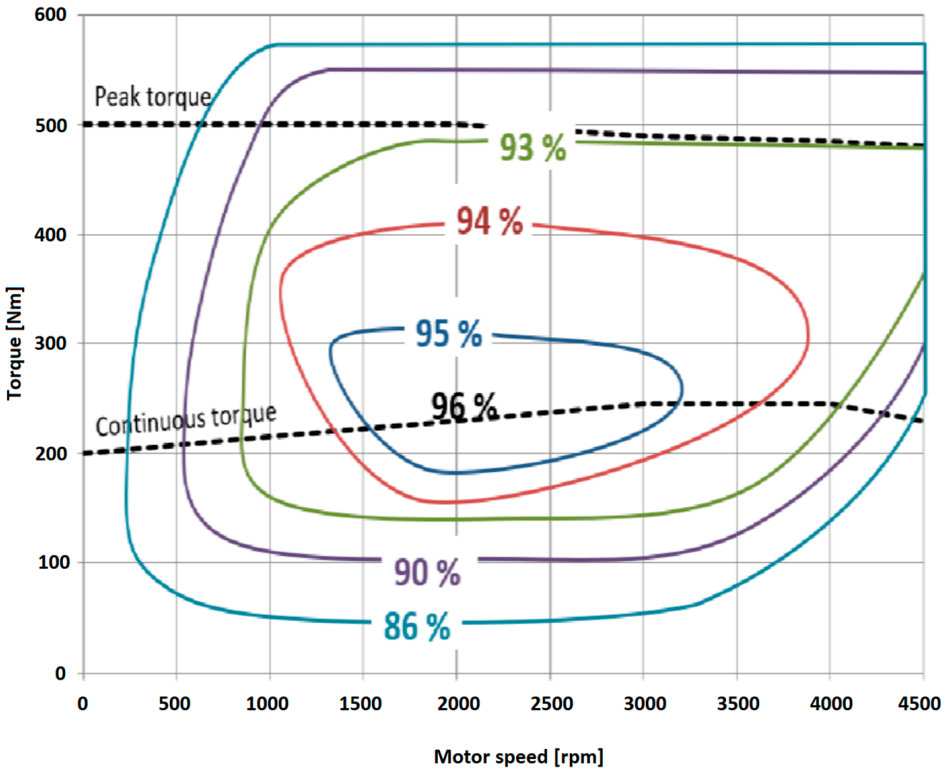

Figure 11. Efficiency of the EMRAX268 motor [38].

Both the propeller PMSM EMRAX228 motors and the electric generator PMSM EMRAX268 motor are controlled by DTI Drivetrain Innovation HV-500 inverters [45] (Table 4), with a separate inverter designated for each motor. The propellers can be controlled in two modes of operation: requested RPM or requested torque, and this set value is controlled by an inbuilt inverter PID controller. The generator inverter controls the PMSM motor, producing energy to supply the propeller motors and battery charging. Motor inductance is used to boost the voltage in a controlled way, ensuring control over the (battery) charging process, i.e., in constant power or constant current mode. There is a DC servo used to control the ICE throttle and consequently to provide mechanical energy to be converted into electric current. The performance parameters of both the ICE and the HV-500 inverter are

calculated by the system's main control unit. Communication between all inverters and the main aircraft control unit is provided via the CAN network, where CANopen is deployed as the communication protocol. There are two types of HV-500 inverters used in this system, with the only difference being the cooling system. The propeller inverters are air-cooled, whereas the generator inverter is liquid-cooled. Other properties remain the same for both the generator and propeller inverters. Even if liquid-cooled inverters require just 0.1 L of coolant within the device, the size and weight of the complete liquid-cooling system resulted in the design decision to use liquid-cooled devices only in generator sub-system, where air flow cannot be guaranteed, especially during ground operations. Thus, in the generator sub-system where ICE requires liquid-cooling anyway, it was also selected for the EMRAX PMSM motor and DTI inverter. For efficiently removing the heat resulting from losses in the inverter, a coolant flow of 19 L/m (liters per minute) is required at the temperature of maximum 60 °C at input and the pressure of minimum value of 1.25 bar (whereas a 2 bar maximal pressure is permitted).

Table 4. Selected parameters for the HV-500 inverter [45].

Parameter	Value
High voltage input range	200–800 V
High voltage maximum input current	350 A
Continuous AC current (peak-to-peak current)	400 $A_{pk\text{-}pk}$
Maximum AC current for short period (peak-to-peak current)	500 $A_{pk\text{-}pk}$
Maximum AC current for short period (RMS)	350 A_{rms}
Switching frequency	8–14 kHz
Maximum electric RPM	100,000 eRPM
Typical efficiency	95%

The experimental ground setup (Figures 12 and 13) consists of additional modules to facilitate a wide range of measurements and control of the testing program at the research and development stage of the project. This includes a power supply that imitates a battery set. This extra equipment is not to be installed onboard the target experimental aircraft to be tested in flight. Its only purpose is to provide more channels for monitoring and measurement during ground tests prior to in-flight testing. The simulated aircraft's main control unit is a single-board computer (SBC) running the Linux operating system. In the diagram, it is referred to as eFADEC as it is digital and controls the electric power generator engine, as well as electric motors driving the propellers, and there are no mechanical means to bypass the direct digital (by-wire) controls. With the propellers being driven by PMSM motors controlled by inverters via the CAN interface, a mechanical link control is out of scope in any case. There are concerns about using a Linux-based single-board computer to control the power plant for the target to flight test the experimental aircraft. Therefore, the next iteration of the project involves the use of a dedicated, microcontroller-based ECU, which can be much more reliable and would justify a more conservative approach. At this stage, using a Linux-based environment allows for rapid development deploying agile methods, with flexible development tools available for both the front-end and back-end parts of the controlling software. The target eFADEC module for subsequent tests is designed around the STM32F7 microcontroller, which allows for real-time operations, high computational power and a wide adaptation of required peripherals and communication links.

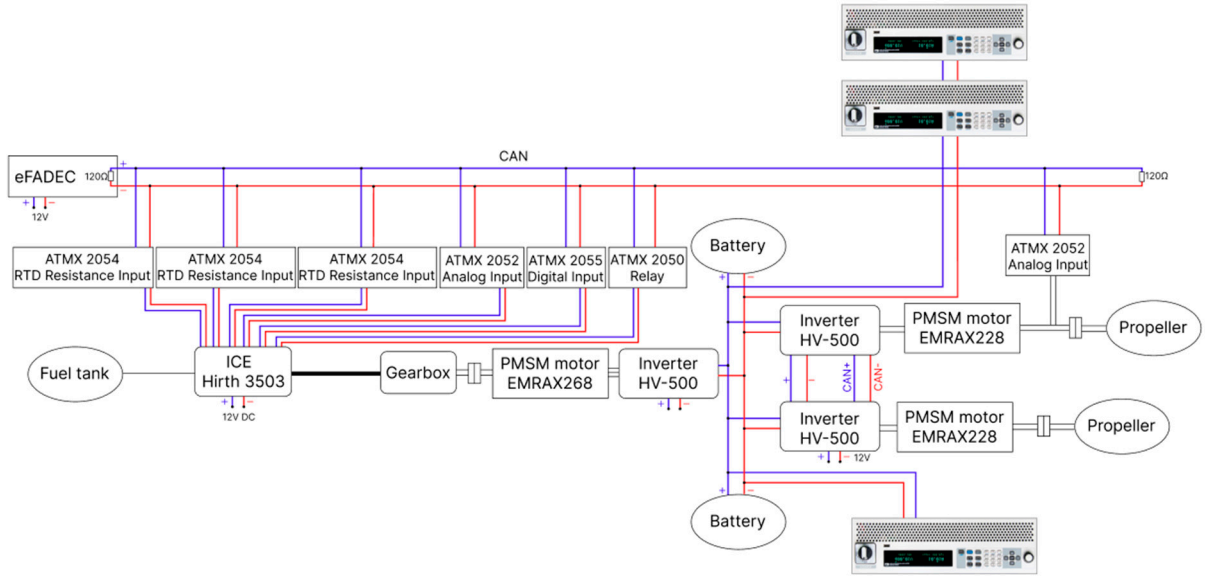

Figure 12. Architecture of the PW-X20 propulsion system ground testbed.

Figure 13. Ground testbed of the PW-X20 propulsion system.

5. Conclusions

With respect to air traffic growth, in-flight emissions and community noise are a major challenge to aircraft design, up to now essentially addressed with incremental improvements in aerodynamics, engine technology and operations. In order to dramatically reduce the carbon footprint of aviation for an environmentally friendly air transport system,

alternative propulsion concepts are one of the promising fields for research and first applications. In this context, the objective of the integration of a hybrid-electric propulsion system in a suitable airframe is to increase efficiency while reducing in-flight emissions, reduce community noise and at the same time provide a viable operating cost and increase reliability. All of the work, up to now mainly focused on smaller general aviation airplanes, can demonstrate the effects of hybrid-electric architectures on key factors such as fuel consumption, noise and maintenance efforts and at the same time will help to de-risk the development of larger aircraft, which, once in operation, will have a more significant environmental impact. Research on general aviation airplanes will also help to develop a new generation of trainer airplanes. Despite the development of flight simulator technology, training on small airplanes is still the most effective method of training pilots of commercial passenger aircraft. Therefore, the fleet of small airplanes will remain large until unmanned commercial aircraft can carry passengers. Unfortunately, outdated piston engines designed in the 1950s (with minor modifications) still power the propellers of many small aircraft used for training. All of these airplanes can be replaced with new ones with the advanced propulsion systems currently developed and tested. This will not only drive down general aviation emissions but also teach pilots how to use these new propulsion systems. This knowledge will then be useful in the course of pilots' careers in commercial aviation.

This paper illustrates an inexpensive approach to the research on small, manned aircraft with a hybrid fuel–electric propulsion system. It was demonstrated that a small experimental propulsion system of that kind can be installed on a two-seater aerobatic glider without significant structural modifications and still comply with the most important points of the CS-22 airworthiness regulations. Mass analysis was performed to check how much heavier the hybrid-motorized glider will be in reference to its aerobatic original. This analysis also allowed us to distribute components of the propulsion system in such a way that the original CoM limits are not exceeded. Aerodynamic analysis was performed to investigate the drag increase due to the installation of additional equipment. Both of these analyses were used to estimate the aerodynamic performance of the new design. It was then decided that the propulsion system would consist of a power generator (Hirth 3505 ICE and Emrax 268 LV-CC), two Emrax 228 HV-AC driving propellers and three HV-500 inverters, one for each motor. The performance of the glider with this propulsion system was analyzed for various propulsion operations modes, proving that a safe flight testing program can be performed. Finally, loads analysis indicated that only small modifications of the wing structure are necessary to use the new design in the utility category.

It is envisaged that the propulsion system will undergo a series of ground tests before its installation on the flying platform. In order to perform these tests, a ground testbed was designed and built. It is believed that a thorough investigation of the propulsion system on the ground will reveal both the advantages and disadvantages of the system. This should facilitate the successful installation of the system under study on a flying aircraft.

Author Contributions: Conceptualization, C.G.; methodology, A.K.; software, R.G.; validation, C.G. and A.S.; formal analysis, A.K.; investigation, A.K.; resources, R.G.; data curation, A.K.; writing—original draft preparation, A.K., R.G., A.S. and C.G.; writing—review and editing, A.K., R.G., A.S. and C.G.; visualization, A.K.; supervision, C.G.; project administration, C.G.; funding acquisition, C.G. All authors have read and agreed to the published version of the manuscript.

Funding: This research was funded by the Warsaw University of Technology under the Excellence Initiative: Research University (IDUB) Program (grant number: 1820/59/Z01/2021).

Data Availability Statement: Data sharing within the article.

Acknowledgments: We thank EMRAX INNOVATIVE E-MOTORS who allowed us to use their figures cited in this paper. Many thanks are also due to Adam Żarnoch, who helped us to improve the language of this paper.

Conflicts of Interest: The authors declare no conflict of interest.

References

1. European Commission. *The European Green Deal*; EC, European Union: Maastricht, The Netherlands, 2019.
2. ACARE. *Fly the Green Deal, Europe's Vision for Sustainable Aviation, Report of the Advisory Council for Aviation Research and Innovation in Europe (ACARE)*; EC RTD; European Union: Maastricht, The Netherlands, 2022.
3. Siemens. World's First Serial Hybrid Electric Aircraft to Fly at Le Bourget. Press Release, 20 June 2011. Available online: https://press.siemens.com/global/en/pressrelease/worlds-first-serial-hybrid-electric-aircraft-fly-le-bourget (accessed on 19 October 2023).
4. Boric, M. Magnus eFusion Rolls out at AERO Friedrichshafen. Flying (Online). 21 April 2016. Available online: https://www.flyingmag.com/magnus-efusion-rolls-out-at-aero-friedrichshafen/ (accessed on 11 November 2023).
5. Perkon. HYPSTAIR—An Introduction to the Project. e2Flight Symposium 2016, Stuttgart. Available online: http://www.hypstair.eu/hypstair-at-symposium-e2-flying-stuttgart-18th-19th-february-2016/ (accessed on 19 October 2023).
6. Gaspari, F.; Trainelli, L.; Rolando, A.; Perkon, I. D1.1: Concept of Modular Architecture for Hybrid Electric Propulsion of Aircraft. December 2017. Available online: https://mahepa.eu/result/ (accessed on 19 October 2023).
7. Lay, J.; Strohmayer, A. Implementation of a 2-seat hybrid electric aircraft demonstrator for reducing carbon emissions. In *International Symposium on Electric Aviation and Autonomous Systems (ISEAS)*; Springer: Cham, Switzerland, 2022.
8. Lay, J.; Bender, A.; Strohmayer, A. Layout and testing of a serial hybrid electric powertrain for a light twin demonstrator platform. *IOP Conf. Ser. Mater. Sci. Eng.* **2021**, *1226*, 012068. [CrossRef]
9. Pope, S. Diamond Flies Multi-Engine Hybrid-Electric Prototype. Flying (Online). 20 November 2018. Available online: https://www.flyingmag.com/diamond-da40-hybrid-electric-prototype-flies/ (accessed on 11 November 2023).
10. Schiff, B. Ampaire 337 'Parallel Hybrid' Unveiled. AOPA (Online). 10 June 2019. Available online: https://www.aopa.org/news-and-media/all-news/2019/june/10/ampaire-337-parallel-hybrid-unveiled (accessed on 11 November 2023).
11. Wildes, M. Ampaire Eco Caravan Conducts First Flight. Flying. 21 November 2022. Available online: https://www.flyingmag.com/ampaire-eco-caravan-conducts-first-flight/ (accessed on 19 October 2023).
12. Sampson, B. VoltAero Cassio Hybrid-Electric Aircraft to Pass 10,000 km Milestone. Aerospace Testing, April 2022. Available online: https://www.aerospacetestinginternational.com/news/electric-hybrid/voltaero-cassio-hybrid-electric-aircraft-to-pass-10000km-flown-milestone.html (accessed on 21 November 2023).
13. Warwick, G. *Canada's NRC Flies Cessna As Hybrid-Electric Testbed*; Aviation Week. 6 April 2022. Available online: https://aviationweek.com/aerospace/advanced-air-mobility/canadas-nrc-flies-cessna-hybrid-electric-testbed (accessed on 21 November 2023).
14. Lapena-Rey, N.; Mosquera, J.; Bataller, E.; Orti, F. First Fuel-Cell Manned Aircraft. *J. Aircr.* **2010**, *47*, 1825–1835. [CrossRef]
15. Sampson, B. German Hydrogen Aircraft HY4 Claims Altitude Record. Aerospace Testing International (Online). 25 April 2022. Available online: https://www.aerospacetestinginternational.com/news/electric-hybrid/german-hydrogen-aircraft-hy4-claims-altitude-record.html (accessed on 11 November 2023).
16. Perry, D. ZeroAvia Flies Do 228 Solely Using ZA600 Powertrain as Testbed Makes Third Flight. FlightGlobal (Online). 24 March 2023. Available online: https://www.flightglobal.com/air-transport/zeroavia-flies-do-228-solely-using-za600-powertrain-as-testbed-makes-third-flight/152618.article (accessed on 11 November 2023).
17. Hemmerdinger, J.; Hardee, H. Universal Hydrogen Completes First Flight of Hydrogen-Powered Dash 8. FlightGlobal. 2 March 2023. Available online: https://www.flightglobal.com/airframers/universal-hydrogen-completes-first-flight-of-hydrogen-powered-dash-8/152306.article (accessed on 19 October 2023).
18. Brelje, B.J.; Martins, J.R.R.A. Electric, hybrid, and turboelectric fixed-wing aircraft: A review of concepts, models, and design approaches. *Prog. Aerosp. Sci.* **2019**, *104*, 1–19. [CrossRef]
19. Xie, Y.; Savvarisal, A.; Tsourdos, A.; Zhang, D.; Gu, J. Review of hybrid electric powered aircraft, its conceptual design and energy management methodologies. *Chin. J. Aeronaut.* **2021**, *34*, 432–450. [CrossRef]
20. Salem, K.A.; Palaia, G.; Quarta, A.A. Review of hybrid-electric aircraft technologies and designs: Critical analysis and novel solutions. *Prog. Aerosp. Sci.* **2023**, *141*, 100924. [CrossRef]
21. Kuśmierek, A.; Galński, C.; Stalewski, W. Review of the hybrid gas—Electric aircraft propulsion systems versus alternative systems. *Prog. Aerosp. Sci.* **2023**, *141*, 100925. [CrossRef]
22. Salem, K.A.; Cipolla, V.; Palaia, G.; Binante, V.; Zanetti, D. Conceptual study of hybrid-electric box-wing aircraft towards the reduction of aviation effects on local air quality and climate change. In Proceedings of the 33rd Congress of the International Council of the Aeronautical Sciences, Stockholm, Sweden, 4–9 September 2022.
23. Fouda, M.; Adler, E.J.; Bussemaker, J.H.; Martins, J.R.R.A.; Kurtulus, D.F.; Boggero, L.; Nagel, B. Automated hybrid propulsion model construction for conceptual aircraft design and optimization. In Proceedings of the 33rd Congress of the International Council of the Aeronautical Sciences, Stockholm, Sweden, 4–9 September 2022.
24. Andrews, C.; Simpson, A. Hybrid electric propulsion development for commercial aviation. In Proceedings of the 33rd Congress of the International Council of the Aeronautical Sciences, Stockholm, Sweden, 4–9 September 2022.
25. Avanzini, G.; Bernardini, G.; Moretti, S.; Serafini, J. Series-Hybrid Retrofit of An Xv-15 Tiltrotor and Emergency Procedure Energetic Analysis. In Proceedings of the 33rd Congress of the International Council of the Aeronautical Sciences, Stockholm, Sweden, 4–9 September 2022.

26. Batra, A.; Raute, R.; Camilleri, R. Series or parallel hybrid-electric aircraft propulsion systems? Case studies of the atr42 and atr72. In Proceedings of the 33rd Congress of the International Council of the Aeronautical Sciences, Stockholm, Sweden, 4–9 September 2022.
27. Bohnert, P.; Ying, S.X.; Selier, M. Demonstration flights of hybrid electric aircraft. In Proceedings of the 33rd Congress of the International Council of the Aeronautical Sciences, Stockholm, Sweden, 4–9 September 2022.
28. Nicolosi, F.; Marciello, V.; Cusati, V.; Orefice, F. Technology roadmap and conceptual design of hybrid and electric configurations in the commuter class. In Proceedings of the 33rd Congress of the International Council of the Aeronautical Sciences, Stockholm, Sweden, 4–9 September 2022.
29. Marciello, V.; Ruocco, M.; Nicolosi, F.; Di Stasio, M. Market analysis, tlars selection and preliminary design investigations for a regional hybrid-electric aircraft. In Proceedings of the 33rd Congress of the International Council of the Aeronautical Sciences, Stockholm, Sweden, 4–9 September 2022.
30. Available online: https://en.wikipedia.org/wiki/Politechnika_Warszawska_PW-6 (accessed on 19 October 2023).
31. Pope, A. *Wind-Tunnel Testing*; John Wiley & Sons, Inc.: New York, NY, USA, 1947; p. 132.
32. Abbot, H.; von Doenhoff, A.E. *Theory of Wing Sections*; Dover Publications, Inc.: New York, NY, USA, 1959; p. 156.
33. Torenbeek, E.; Wittenberg, H. *Flight Physics*; Springer: Dordrecht, The Netherlands; Berlin/Heidelberg, Germany; London, UK; New York, NY, USA, 2009; p. 152.
34. Nicolay, L.M.; Carichner, G. *Fundamentals of Aircraft and Airship Design*; AIAA, Inc.: Reston, VA, USA, 2010; Volume 1, p. 178.
35. Marjanowski, J.; Tomasiewicz, J.; Frączek, W. *The Electric-Powered Motorglider AOS-71—The Study of Development*; Aircraft Engineering and Aerospace Technology: Bradford, UK, 2017; Volume 89, pp. 579–589.
36. CS-22 Airworthiness Regulation. Available online: https://www.easa.europa.eu/en/document-library/certification-specifications/group/cs-22-sailplanes-and-powered-sailplanes (accessed on 21 November 2023).
37. Available online: https://hirthengines.com/wp-content/uploads/3503-brochure-soft-copy.pdf (accessed on 19 October 2023).
38. EMRAX_228_datasheet_v1.5. Available online: https://emrax.com/e-motors/emrax-228/#1482059435741-232ed37a-accc (accessed on 22 November 2023).
39. EMRAX_268_datasheet_v1.5. Available online: https://emrax.com/e-motors/emrax-268/ (accessed on 22 November 2023).
40. Available online: https://www.alldatasheet.com/datasheet-pdf/pdf/1643878/SONY/US18650VTC6.html (accessed on 19 October 2023).
41. Rodzewicz, M.; Sierputowski, P. EB-2—The Fly Lab of the Warsaw University of Technology. *Tech. Soar.* **2009**, *33*, 66–71. [CrossRef]
42. Rodzewicz, M.; Głowacki, D. The EB-3 Fly-Lab of the Warsaw University of Technology. *Arch. Mech. Eng.* **2012**, *LIX*, 175–198. [CrossRef]
43. Available online: https://en.wikipedia.org/wiki/Politechnika_Warszawska_PW-4_Pelikan (accessed on 19 October 2023).
44. Available online: https://www.galaxysky.cz/grs-6-750-sds-ff-140m2-p42-pl (accessed on 19 October 2023).
45. Available online: https://drivetraininnovation.com/products (accessed on 19 October 2023).